Chapter 3
Photon Transfer Noise Sources

When photons strike a detector, interactions immediately produce a signal variance or *noise* from pixel-to-pixel. This chapter introduces four fundamental noise sources important to PT work. The first two sources, *signal shot noise* and *Fano noise*, are related to photon interaction. The third noise source, *fixed pattern noise*, is associated with pixel-to-pixel sensitivity nonuniformity. The fourth source, *read noise*, encompasses all other noise sources that are not dependent on signal strength. Shot noise increases by the square root of signal, whereas FPN increases proportionally with signal. Fano noise increases by the square root of photon energy (or quantum yield).
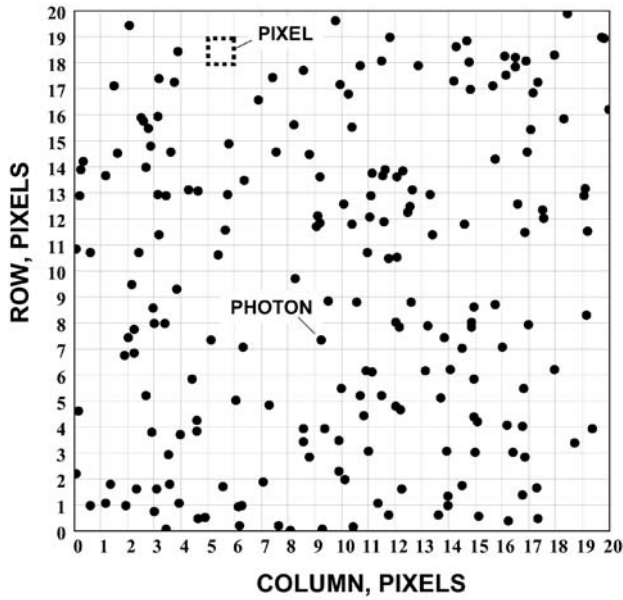
3.1 Photon Shot Noise

Signal shot noise is fundamentally connected to the way photons spatially arrive on a detector. For example, Fig. 3.1 shows a Monte Carlo simulation where 200 photons are randomly interacting with a 20×20 pixel region. As can be seen, the number of photon interactions varies from zero to four interactions per pixel. The standard deviation (or rms) for the number of interactions per pixel is called *photon shot noise*.

Photon shot noise—a spatially and temporally random phenomenon described by Bose-Einstein statistics—is expressed by

$$\sigma_{\mathrm{SHOT}}(P_{\mathrm{I}})^2 = P_{\mathrm{I}} \frac{e^{hc/\lambda kT}}{e^{hc/\lambda kT} - 1},\tag{3.1}$$

where $\sigma_{\mathrm{SHOT}}(P_{\mathrm{I}})^2$ is the interacting photon shot noise variance, h is Planck's constant (6.626×10^{-34} J-s), λ is the photon wavelength (cm), k is Boltzmann's constant (1.38×10^{-23} J/K), c is the speed of light (2.99×10^8 m/sec), and T is absolute temperature (K).

Figure 3.2 plots Eq. (3.1) as a function of wavelength (μm) and the temperature of the semiconductor. For wavelengths greater than 10 μm, photons couple with phonons (i.e., lattice vibrations in a solid) that increase the shot noise. As the operating temperature is reduced, the semiconductor produces less coupling action and variance as seen in the plot. However, for silicon detectors this phenomenon is not observed since the photoelectric effect for wavelengths >1 μm can not take

Figure 3.1 Monte Carlo simulation showing photons interacting with pixels.
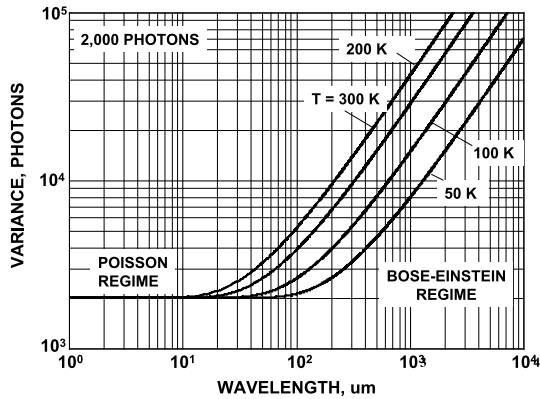
Figure 3.2 Photon shot noise variance as a function of wavelength.

place. Assuming that $hc/\lambda \ll kT$, Eq. (3.1) reduces to the familiar shot noise relation characteristic of visible imagers as

$$\sigma_{\mathrm{SHOT}}(P_{\mathrm{I}}) = P_{\mathrm{I}}^{1/2}. \tag{3.2}$$

Photon shot noise is described by the classical Poisson probability distribution,

$$p_i = \frac{P_{\mathrm{I}}^i}{i!} e^{-P_{\mathrm{I}}}, \tag{3.3}$$

where p_i is the probability that there are i interactions per pixel.

═══════════

Example 3.1

Find the probability that 0, 1, 2, and 3 photons interact with a pixel, assuming an average of 1 interacting photon per pixel.

Solution:
From Eq. (3.3):

$$p_0 = \frac{1^0}{0!}e^{-1} = 0.368 \quad \text{0 photon interactions}$$

$$p_1 = \frac{1^1}{1!}e^{-1} = 0.368 \quad \text{1 photon interaction}$$

$$p_2 = \frac{1^2}{2!}e^{-1} = 0.184 \quad \text{2 photon interactions}$$

$$p_3 = \frac{1^3}{3!}e^{-1} = 0.0613 \quad \text{3 photon interactions}$$

Figure 3.3 shows results from a random number generator governed by Poisson statistics. The histogram plots occurrences as a function of interacting photons per pixel, assuming 90,000 pixels and 90,000 interacting photons (i.e., $P_I = 1$). The resultant distribution follows the Poisson formula given by Eq. (3.3). For example, 33,200 pixels have one photon interaction, whereas 33,070 pixels show no interactions. The results are expanded and plotted in Fig. 3.4 on a log curve that shows six pixels with seven events.

═══════════

Figure 3.3 also shows a Gaussian curve to fit data for Example 3.1 that follows
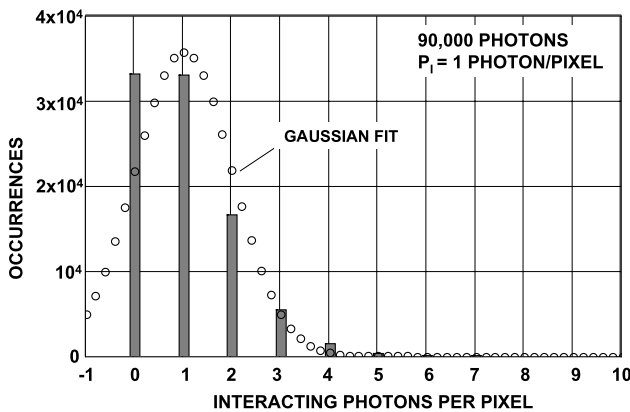
Figure 3.3 Interacting-photons-per-pixel histogram for Fig. 3.1 assuming 1 photon/pixel average.
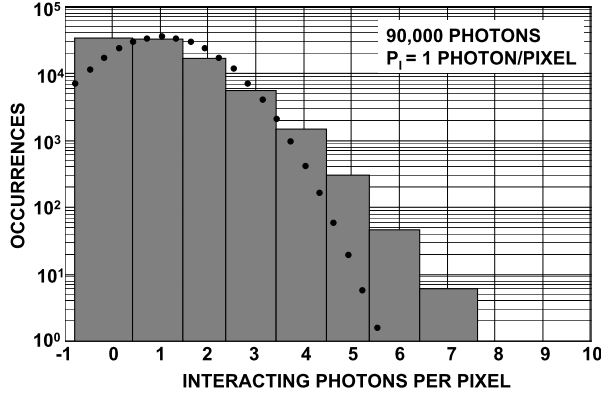
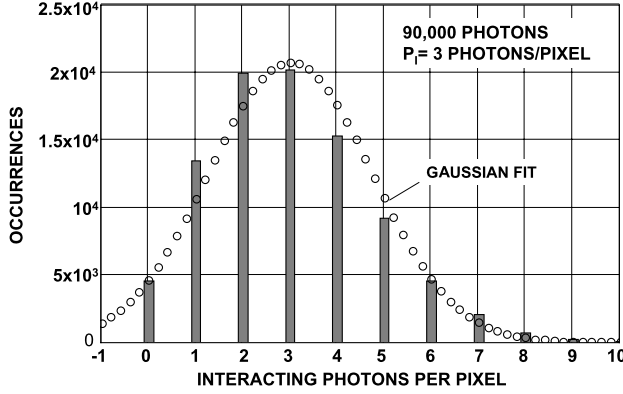**Figure 3.4** Logarithmic histogram for Fig. 3.3.

Figure 3.5 Interacting-photons-per-pixel histogram assuming 3 photons/pixel average.

the relation

$$p_i = \frac{1}{(2\pi)^{1/2}\sigma_{\mathrm{PI}}} e^{-(i-P_{\mathrm{I}})^2/2\sigma_{\mathrm{PI}}^2}. \tag{3.4}$$

A Gaussian distribution approximates a Poisson distribution when the number of interacting photons per pixel is large. For example, Fig. 3.5 is a histogram plot that assumes $P_{\mathrm{I}} = 3$, which exhibits a better fit to the Poisson distribution. Figure 3.6 is a histogram for $P_{\mathrm{I}} = 20$ and shows a near-perfect normal distribution.
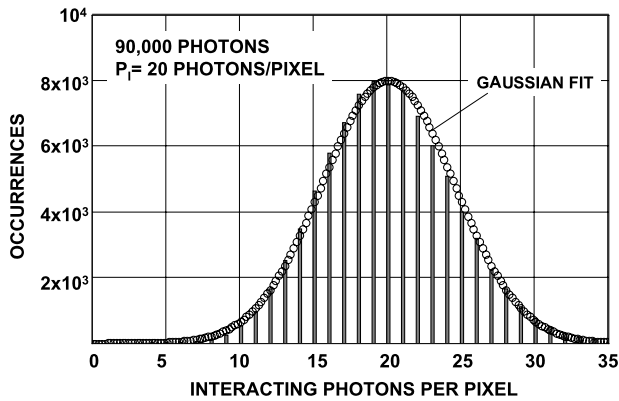
3.2 Signal Shot Noise

The signal shot noise generated by interacting photons is given by

$$\sigma_{\mathrm{SHOT}} = \eta_{\mathrm{i}}(P_{\mathrm{I}})^{1/2}, \tag{3.5}$$

where σ_{SHOT} is the signal shot noise (rms e$^-$). Substituting Eq. (2.8) into Eq. (3.5) yields

$$\sigma_{\mathrm{SHOT}} = (\eta_{\mathrm{i}}S)^{1/2}. \tag{3.6}$$

Figure 3.6 Interacting-photon-per-pixel histogram assuming 20 photons/pixel average.

Equation (3.6) is used extensively throughout this book. The relation will be verified through simulation in Figs. 3.9–3.11.

Example 3.2

Assume from Example 3.1 that each interacting photon generates an electron. Add random noise to the response histogram shown in Fig. 3.3 to produce histograms for the following noise levels: 0.1, 0.2, 0.3, 0.4, and 0.5 e⁻ rms.

Solution:

Figure 3.7 shows the desired histograms. Note that the noise degrades the resolution between electron peaks. Although some CCD and CMOS imagers exhibit read noise levels slightly less than 1 e⁻, the noise level is still too high to resolve single-photon interactions. Is it coincidental that the detector's noise level is just shy of doing this?


3.3 Fano Noise

If all the energy of an interacting photon was spent in the production of electron-hole (e-h) pairs, then there would be no variation in the number of e-h pairs produced. On the other hand, if the energy was partitioned between breaking covalent bonds and lattice vibrations, or if phonon production was uncorrelated, Poisson statistics would apply. But neither is the case in nature. The variance in multiple electron-hole charge generation, called *Fano noise*, is empirically described by

$$\sigma_{\text{FN}} = (F_{\text{F}} \eta_{\text{i}})^{1/2} = \left(F_{\text{F}} \frac{h_\nu}{E_{\text{e-h}}} \right)^{1/2}, \tag{3.7}$$

where σ_{FN} is the Fano noise (e⁻ rms), and F_{F} is referred to as the *Fano factor*, which is defined by the variance in the number of electrons generated divided by
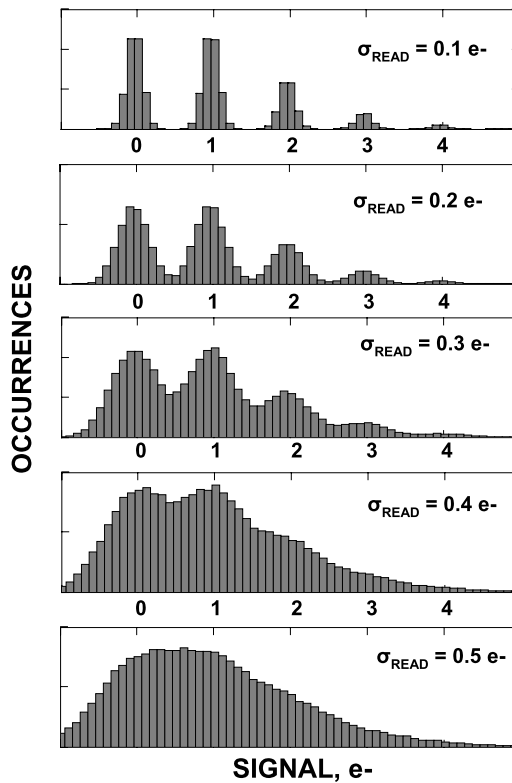
Figure 3.7 Histograms showing influence of different read noise levels on Fig. 3.3.

the average number of electrons generated per interacting photon. The Fano factor is approximately 0.1 for silicon and is applicable for photon energies greater than 10 eV. Figure 3.8 plots Fano noise as a function of photon energy and wavelength. Note that Fano noise becomes appreciable in the soft x-ray regime (i.e., when greater than the read noise floor of 1 e⁻ rms). Ultra-low read noise CCD and CMOS imagers and cameras are Fano noise-limited through out the x-ray spectrum (and are referred to as such).
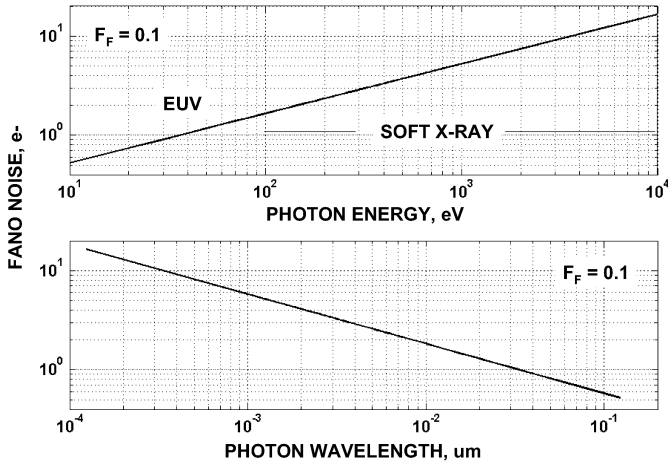
Example 3.3

Determine the Fano noise, assuming a quantum yield of 1620 e⁻ per interacting photon ($h_\nu = 5.9$ keV).

Solution:
From Eq. (3.7),

$$\sigma_{\mathrm{FN}} = (0.1 \times 1620)^{1/2} = 12.7 \ \mathrm{e}^-.$$

**Figure 3.8** Fano noise as a function of photon energy and wavelength.

Figure 3.9 presents a simulation experiment where 90,000 pixels are exposed to an average photon flux of three interacting photons/pixel with $\eta_i = 10\,e^-$/interacting photons. Note that the signal peaks that define the Poisson envelope are separated by $10\,e^-$ at locations given by

$$S_{\text{PEAK}} = N_P \eta_i, \tag{3.8}$$

where S_{PEAK} is the signal charge peak level, and N_P is the number of multiple photon interactions per pixel that take place. For example, $N_P = 4$ produces a signal peak at $40\,e^-$.

The corresponding standard deviation caused by Fano noise about each signal peak is given by

$$\sigma_{\text{FN\_PEAK}} = (N_P F_F \eta_i)^{1/2}. \tag{3.9}$$
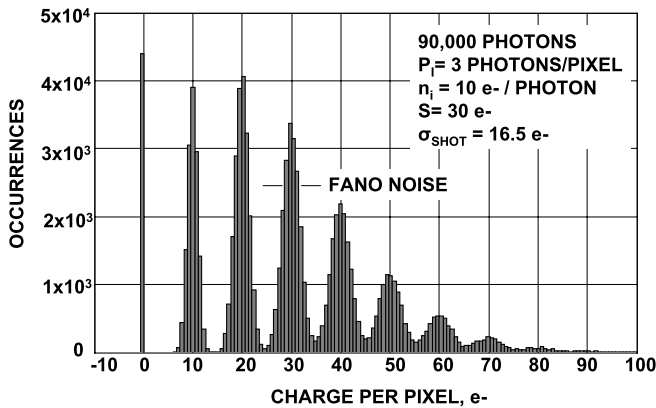
Figure 3.9 Charge-generated-per-pixel histogram with Fano noise present ($n_i = 10\,e^-$/ photon, $P_I = 3$ photons/pixel).

Note that the noise about each peak increases with N_P because the Fano noise for multiple pixel-photon interactions is added in quadrature by $(N_P)^{1/2}$. This broadening effect is seen in Fig. 3.9, where the separation between signal peaks is less pronounced. Figure 3.10 shows a similar histogram where the average photon flux rate is increased from three to 10 interacting photons/pixel. Note that the signal peaks are unresolved for large N_P because of Fano noise. Figure 3.11 shows how the resolution improves when the quantum yield is increased from 10 to 30 electrons/interacting photon.

When signal shot noise and Fano noise are added in quadrature, the net noise is
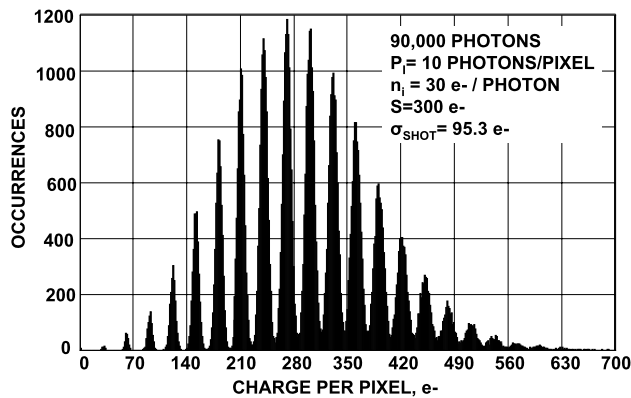
$$\sigma_{SHOT+FN} = (\sigma_{SHOT}^2 + \sigma_{FN}^2)^{1/2}. \tag{3.10}$$

Substituting Eqs. (3.6) and (3.7) into Eq. (3.10) yields

$$\sigma_{SHOT+FN} = (\eta_i(S + F_F))^{1/2}. \tag{3.11}$$
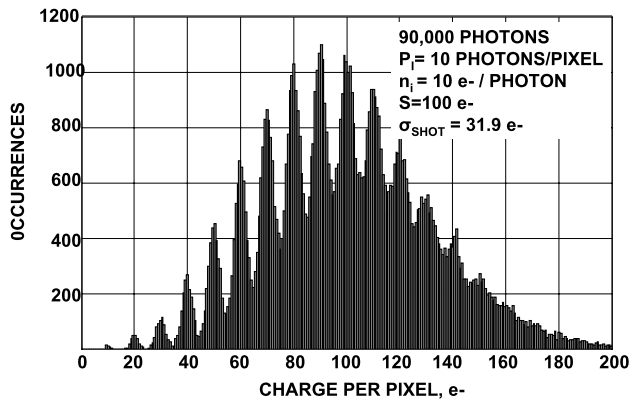
Figure 3.10 Charge-generated-per-pixel histogram with Fano noise ($n_i = 10$ e$^-$/photon, $P_I = 10$ photons/pixel).

Figure 3.11 Charge-generated-per-pixel histogram with Fano noise ($n_i = 30$ e$^-$/photon, $P_I = 10$ photons/pixel).